

$S(q, \omega)$ for the $S = \frac{1}{2}$ and $S = 1$ one-dimensional Heisenberg antiferromagnet: A quantum Monte Carlo study

J. Deisz, M. Jarrell, and D. L. Cox

Department of Physics, The Ohio State University, Columbus, Ohio 43210

(Received 10 May 1990)

The dynamic-spin-correlation function $S(q, \omega)$ is computed for the one-dimensional antiferromagnetic Heisenberg model for $S = \frac{1}{2}$ and $S = 1$. Imaginary-time correlation functions are evaluated with the quantum Monte Carlo method and the maximum-entropy method is used to continue these results to real frequencies. This technique produces a value for the $S = 1$ Haldane gap that agrees with previous work and also gives a good description of inelastic neutron scattering data for the one-dimensional $S = \frac{1}{2}$ antiferromagnet $\text{CuCl}_2 \cdot 2\text{N}(\text{C}_5\text{D}_5)$.

The dynamics of the one-dimensional antiferromagnetic Heisenberg model, described by

$$H = J \sum_{i=1}^N \mathbf{S}(R_i) \cdot \mathbf{S}(R_{i+1}), \quad J > 0, \quad (1)$$

has been of considerable interest since Haldane made the novel prediction that when the number of sites N becomes infinite the excitation spectrum for integer spins is gapped, in contrast to the excitation spectrum for half-integer spins which is gapless.¹ This model is also of experimental relevance as $\text{CuCl}_2 \cdot 2\text{N}(\text{C}_5\text{H}_5)$ ($S = \frac{1}{2}$) and CsNiCl_3 ($S = 1$) are examples of nearly one-dimensional antiferromagnets.

This paper will describe the calculation of $S(q, \omega)$, the dynamic spin correlation function using quantum Monte Carlo and the maximum entropy method. $S(q, \omega)$ is given by

$$S(q, \omega) = \frac{\pi}{Z} \sum_{m,n} e^{-\beta E_m} \langle m | S_z(q) | n \rangle \langle n | S_z(-q) | m \rangle \times \delta[\omega - (E_n - E_m)], \quad (2a)$$

where

$$S_z(q) = N^{-1/2} \sum_{i=1}^N e^{-iqR_i} S_z(R_i), \quad (2b)$$

which shows that $S(q, \omega)$ describes excitations from the thermal equilibrium state. $S(q, \omega)$ is important experimentally because it is directly measured in inelastic neutron-scattering experiments.

There has been considerable work done on the dynamical properties of one-dimensional Heisenberg antiferromagnets. Müller, Beck, and Bonner² have produced a zero-temperature ansatz for $S(q, \omega)$ when $S = \frac{1}{2}$ which is consistent with exact sum rules within factors of order unity. Most studies have been restricted to determining the lowest-lying excited states because full matrix diagonalization is prohibitive for reasonable size systems. The dispersion relation for the lowest-lying triplets for $S = \frac{1}{2}$ in the thermodynamic limit is given by $\varepsilon(q) = (\pi/2)J \sin(q)$,³ thus gaplessness for $S = \frac{1}{2}$. So $S \geq 1$ studies are important in verifying Haldane's prediction. For $S = 1$ Nightingale and Blöte⁴ produced an estimate for the gap Δ of $0.41J$ by extrapolating the results from finite-size

systems (up to 32 sites) to the thermodynamic limit.

Other studies have focused on the equal-time spin-spin correlation function, $S(R) = \langle S_z(R) S_z(0) \rangle$. This correlation function indirectly describes the excitation spectra since a power-law decay of $S(R)$ as a function of R implies gapless excitations and an exponential decay results from gapped excitations. Liang's⁵ zero-temperature calculations and Marcu's⁶ finite-temperature calculation agree with Haldane's prediction, but no estimate for Δ could be produced.

These and other results have been useful in understanding the dynamics of the one-dimensional antiferromagnetic Heisenberg model, but it remains desirable to obtain the temperature-dependent $S(q, \omega)$. $S(q, \omega)$ contains not only information on the low-lying excitations, but also higher-lying excitations that are observed in neutron-scattering experiments.

The large size of the Hilbert space makes direct evaluation of Eq. (2a) difficult for any reasonable size system. However, $S(q, \omega)$ is related to an imaginary-time correlation function $S(q, \tau)$ via

$$S(q, \tau) = \frac{1}{2\pi} \int_{-\infty}^{\infty} e^{-\omega\tau} S(q, \omega) d\omega \quad (3a)$$

where

$$S(q, \tau) = \frac{1}{2} \langle e^{H\tau} S_z(q) e^{-H\tau} S_z(-q) \rangle. \quad (3b)$$

We have evaluated $S(q, \tau)$ and the associated covariance matrix using the world-line quantum Monte Carlo method.⁷ In this method the inverse temperature β is broken into several discrete intervals of length $\Delta\tau$ and the noncommutivity between the terms in Eq. (1) is ignored within these intervals. This procedure becomes exact only in the limit $\Delta\tau \rightarrow 0$. The systematic errors due to the finite size of $\Delta\tau$ ($\Delta\tau \leq 0.25/J$) are estimated to be of order 1% from measurements of the energy at low temperature. Monte Carlo sampling errors are found to be less than 1% for small values of τ , but can become larger when τ increases since the magnitude of $S(q, \tau)$ becomes small. The code was tested versus exact diagonalization of four site systems.⁸

Equation (3a) must be inverted to obtain $S(q, \omega)$ from the Monte Carlo results for $S(q, \tau)$. For a finite set of τ

values (with some error at each τ) this inversion is ill defined. Recently Silver, Sivia, and Gubernatis,⁹ have proposed using the maximum-entropy method¹⁰ for inverting relationships like Eq. (3a) that are commonly found between dynamical quantities and imaginary-time correlation functions which can be measured with quantum Monte Carlo simulations. We refer to Ref. 9 for a full discussion of the maximum-entropy method, but we provide a brief sketch of the technique here.

Let $\hat{S}(q, \omega)$ be some trial function for $S(q, \omega)$.

$$L = \sum_{\tau} \frac{[S(q, \tau) - (1/2\pi) \int_{-\infty}^{\infty} e^{-\omega\tau} \hat{S}(q, \omega) d\omega]^2}{(\sigma_{\tau})^2} \quad (4a)$$

describes how close \hat{S} comes to reproducing the Monte Carlo values of $S(q, \tau)$ relative to the measured error bars σ_{τ} on the Monte Carlo values [in practice Eq. (4a) must be modified to describe the correlation between measurements at different τ values¹¹].

$$I = \int_0^{\infty} \left[-\hat{S}(q, \omega) \ln \frac{\hat{S}(q, \omega)}{m(q, \omega)} + \hat{S}(q, \omega) - m(q, \omega) \right] d\omega \quad (4b)$$

is the entropy and generally becomes more negative the further \hat{S} is from a predefined default model $m(q, \omega)$, the solution to which this analysis will default to in the absence of data. The maximum-entropy result for $S(q, \omega)$ is the trial function \hat{S} , which maximizes $\alpha I(\hat{S}, m) - L(\hat{S})$ where the choice of the constant α is made with the method described by Gull and Skilling.¹⁰ Our $S(q, \omega)$'s produced this way are smooth curves in contrast to the δ functions expected for a finite-sized system. The smoothing is effected by convoluting about a given ω with a box function of width $\Delta\omega = 0.05J$ (smaller $\Delta\omega$ produce no change in shape.)

Figure 1 shows the dependence of the results on the default model $m(q, \omega)$. In order to select $m(q, \omega)$, we note that

$$\frac{1}{2\pi} \int S(q, \omega) d\omega = S(q, \tau=0), \quad (5a)$$

$$\frac{2}{\pi} \int \omega^{-1} S(q, \omega) d\omega = \chi(q), \quad (5b)$$

and

$$\frac{1}{2\pi} \int \omega S(q, \omega) d\omega = \frac{-\langle E \rangle}{3N} [1 - \cos(q)] \quad (5c)$$

$$m(q, \omega) = e^{-1} \exp\{-\lambda_0 [1 + \exp(-\beta\omega)]\} \exp\{-\lambda_1 [1 - \exp(-\beta\omega)]\} \exp\{-\lambda_{-1} [1 - \exp(-\beta\omega)] \omega^{-1}\}, \quad (7)$$

which will be called the "informed default model." The $\{\lambda_i\}$ are numerically determined Lagrange multipliers used to enforce the constraints in maximizing the functional of Eq. (6).

The informed default of Fig. 1 was able to reproduce all the $S(q, \tau)$ data despite having the information from only three sum rules. Thus $m(q, \omega)$ was chosen by the Maxent as $S(q, \omega)$ [we find that this often occurs when $m(q, \omega)$ is chosen in this way]. For the flat default model large changes were required to reproduce the data. These

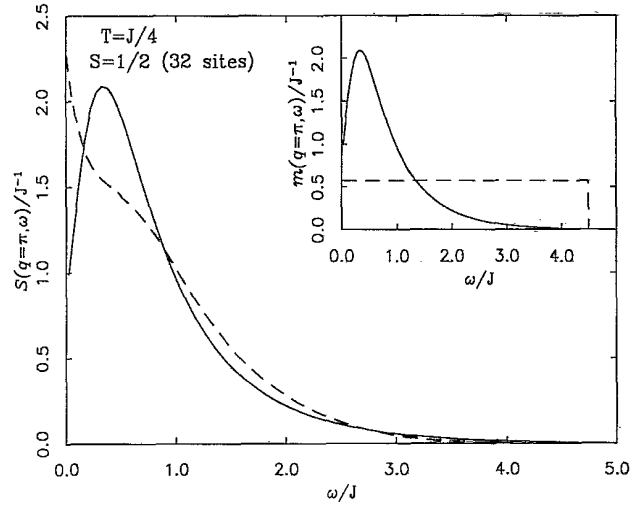


FIG. 1. Dependence on the default model $m(q, \omega)$. The maximum entropy method requires a default model $m(q, \omega)$ so that a unique $S(q, \omega)$ can be chosen which agrees with the imaginary-time correlation function measurements made with quantum Monte Carlo. The default models are plotted in the inset. The broken line was produced with a flat (up to a cutoff at $4.5J$) default model which satisfied only sum rule (5a). The solid line was produced with a default model which satisfied all three sum rules. This latter default model agreed well enough with all imaginary-time data that it became the final result for $S(q, \omega)$. The flat default model contained little information and large changes were required to produce agreement with the Monte Carlo data. Figures 2 and 3 were produced using default models which incorporated the three sum rules.

are three sum rules which should be satisfied by $S(q, \omega)$ (Ref. 12) and whose right-hand sides may be determined by the Monte Carlo technique. It is thus natural to choose an $m(q, \omega)$ which satisfies one or more of these along with the detailed balance constraint $m(q, -\omega) = e^{-\beta\omega} m(q, \omega)$ which we also impose on $S(q, \omega)$. In Fig. 1, the dashed line is for $m(q, \omega)$ flat up to a cutoff at $4.5J$ and normalized to obey (5a). The default model for the full line was chosen by minimizing

$$- \int_0^{\infty} m(q, \omega) \ln[m(q, \omega)] d\omega \quad (6)$$

subject to the constraint that all three sum rules are satisfied.¹³ This produces an $m(q, \omega)$ of the form

changes produced better agreement with the more informed default model, but it was not able to reproduce the low-frequency structure for q near the Brillouin-zone boundary. An error analysis can be used to compare the validity of these two results. It is found that the integrated intensity for $0.1 < \omega < 1.0$ is equal to 0.465 ± 0.013 for the informed default while the flat default model has 0.403 ± 0.143 .¹¹ These results show that the $S(q, \omega)$ produced from the flat default model has too little spectral weight for $0.1 < \omega < 1.0$.

TABLE I. Comparison of the Monte Carlo results for the right-hand sides of (5a)–(5c) compared to the integrals of the left-hand side using the maximum entropy generated $S(q, \omega)$'s. (5a) and (5b) are satisfied to within the statistical accuracy of the Monte Carlo averages. (5c) is satisfied to within 1%, but this is not within the error bars as the energy can be very accurately measured. The default models used to generate these $S(q, \omega)$'s [the $S(q, \omega)$'s are pictured in Fig. 2] incorporated the three sum rules, however default models which do not incorporate these sum rules have similar success in producing $S(q, \omega)$'s which satisfy (5a)–(5c).

Sum	$S = \frac{1}{2}$ ($T = J/8$, 96 sites)		$S = 1$ ($T = J/8$, 64 sites)	
	Monte Carlo	Maximum Entropy	Monte Carlo	Maximum Entropy
$\frac{2}{\pi} \int_{-\infty}^{\infty} \omega^{-1} S(q = \pi, \omega) d\omega$	5.041 ± 0.067	5.017 ± 0.062	18.05 ± 0.20	18.12 ± 0.18
$\frac{1}{2\pi} \int_{-\infty}^{\infty} S(q = \pi, \omega) d\omega$	0.523 ± 0.004	0.522 ± 0.004	2.044 ± 0.014	2.045 ± 0.012
$\frac{1}{2\pi} \int_{-\infty}^{\infty} \omega S(q = \pi, \omega) d\omega$	0.2941 ± 0.0001	0.2948 ± 0.0009	0.9436 ± 0.0008	0.9360 ± 0.0048

Table I compares the results for the right-hand side of (5a)–(5c) evaluated with quantum Monte Carlo to the integrals of the left-hand side using the maximum-entropy method results for $S(q, \omega)$ when $q = \pi$, temperature $= J/8$, and for both $S = \frac{1}{2}$ and $S = 1$ [$S(q, \omega)$'s are shown in Fig. 2]. There is good agreement. Perhaps this is not surprising since the default model incorporated all three sum rules, however, $S(q, \omega)$ is different from the default

model for both of these cases. Further, the three sum rules are reasonably well satisfied even when default models are used which do not incorporate them.¹⁴

Most numerical studies of the Haldane conjecture have focused on $S = \frac{1}{2}$ and $S = 1$ because the Hilbert space increases in size as $(2S+1)^N$ where the system size N must be ≥ 32 to make an accurate prediction of the Haldane gap Δ . World-line Monte Carlo scales like $N \times S$, making

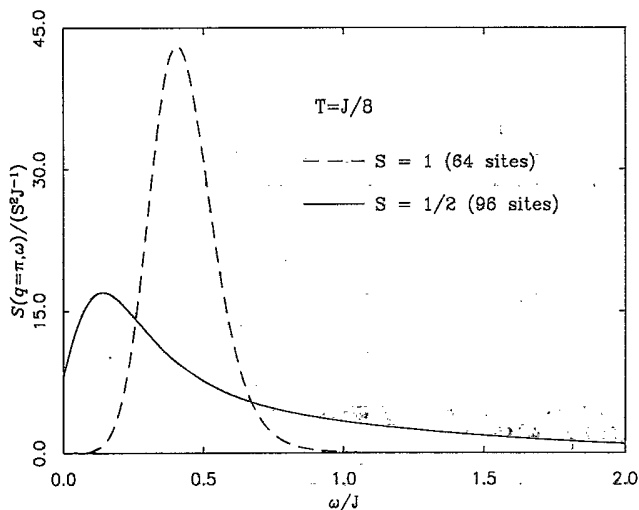


FIG. 2. Comparison of $S(q, \omega)$ for $S = \frac{1}{2}$ and $S = 1$ when $T = J/8$. Haldane has predicted that there is a gap Δ for excitations at zero temperature when $S = 1$, while no gap should be found for $S = \frac{1}{2}$. When $S = \frac{1}{2}$ there is considerably more low-frequency weight than for $S = 1$. If the peak position for $S = 1$ is taken to be Δ , then we obtain $\Delta = 0.41J$ in agreement with previous work (Ref. 4). The peak for $S = \frac{1}{2}$ is not at $\omega = 0$, but the peak moves to zero frequency as temperature decreases; this behavior is not seen when $S = 1$. Note that for $S = 1$ the flat and three sum rule default models discussed for Fig. 1 predict the same peak position in $S(q, \omega)$, but the flat default produces a line shape which is 20% narrower than that produced by the three sum rule default.

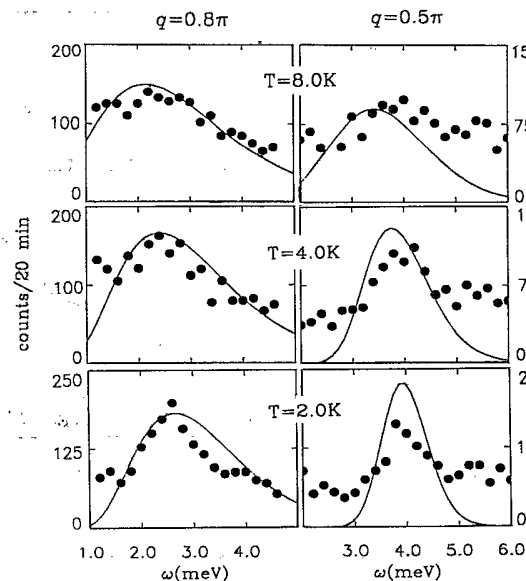


FIG. 3. Inelastic neutron scattering cross section for the one-dimensional antiferromagnet $\text{CuCl}_2 \cdot 2\text{N}(\text{C}_3\text{D}_5)$ vs $(1 - \omega/\epsilon_i)^{1/2} \times S(q, \omega)$ (ϵ_i = incident neutron energy) predicted by quantum Monte Carlo and the maximum entropy method. The solid circles represent the experimental results of Endoh *et al.* (Ref. 15) and the solid lines are our results. The energy scale was set to be 26.8 K by susceptibility and specific-heat measurements. The correct qualitative features are reproduced with the exception that the $q = 0.5\pi$ peak sharpens more quickly with temperature than is observed experimentally.

large values of S accessible; however, here we only consider $S = \frac{1}{2}$ and $S = 1$ to compare with previous results. Also since Δ is expected to be largest for $S = 1$, the simulations can be carried out at high temperatures without the gap structure being eliminated by thermal excitations.

Figure 2 shows $S(q, \omega)$ for $S = \frac{1}{2}$ and $S = 1$ at temperature $J/8$. There are clear differences. When $S = \frac{1}{2}$ there is a broad spectrum with large weight near $\omega = 0$, while the $S = 1$ spectrum is nearly Lorentzian with its peak at $\omega = 0.41J$ and has little low-frequency weight. Indeed, the low-frequency tail is consistent with finite temperature broadening into the gap. If this peak position is taken to be Δ , then our result agrees with that of Nightingale and Blöte who used Green's-function Monte Carlo to project out the ground and lowest-lying excited states of finite chains (up to 32 sites).⁴ They also obtain $\Delta = 0.41J$. $S(q, \omega)$ for $S = \frac{1}{2}$ is not peaked at $\omega = 0$, but the peak position moves closer to $\omega = 0$ when the temperature goes to zero (not shown here). In contrast, the peak position for $S = 1$ does not decrease as temperature is lowered, rather the peak narrows as the temperature is lowered.

Figure 3 is a comparison of our results with inelastic neutron-scattering experiments on $\text{CuCl}_2 \cdot 2\text{N}(\text{C}_5\text{D}_5)$ performed by Endoh *et al.*¹⁵ They determined the energy scale J with susceptibility and specific-heat measurements. Our only fitting parameter is the overall intensity which is set to be the same for both q values and all three temperatures (although there is q dependence from the magnetic structure factor). A direct comparison between

our results and experiment is difficult because of the incoherent background in the experimental data, but the qualitative features of the data are largely reproduced with the exception that the rapid sharpening of our $q = 0.5\pi$ results are not seen experimentally. However, we believe that the agreement is encouraging. Marcu has previously shown that the integrated neutron-scattering cross section agrees well with predictions made with the same Monte Carlo technique used here.¹⁶

In conclusion, we have calculated $S(q, \omega)$ for the $S = \frac{1}{2}$ (up to 96 sites) and $S = 1$ (up to 64 sites) antiferromagnetic Heisenberg models in one dimension using the quantum Monte Carlo method and the maximum-entropy method. Our value for the Haldane gap ($S = 1$) agrees with previous work. Comparison to the inelastic neutron-scattering experiments on $\text{CuCl}_2 \cdot 2\text{N}(\text{C}_5\text{D}_5)$ at finite temperature produced qualitative agreement. It will be interesting to apply this method to higher spin systems ($S = \frac{3}{2}$, $S = 2$) and also to the dynamic spin and charge spectra of the t - J model.

We gratefully acknowledge useful conversations with N. Bonesteel, J. Gubernatis, C. Jayaprakash, D. Scalapino, R. Silver, W. Wenzel, and S. White. This work was supported by NSF Grant No. DMR-8857341 and a grant from the Cray Research Corporation. Allocation of computation time at the Ohio Supercomputer Corporation is gratefully acknowledged. One of us (D.L.C.) thanks the A.P. Sloan Foundation for support.

¹F. D. M. Haldane, Phys. Lett. **93A**, 464 (1983); Phys. Rev. Lett. **50**, 1153 (1983).

²G. Müller, H. Beck, and J. C. Bonner, Phys. Rev. Lett. **43**, 75 (1979).

³J. des Cloizeaux and J. J. Pearson, Phys. Rev. **128**, 2131 (1962).

⁴M. P. Nightingale and H. W. J. Blöte, Phys. Rev. B **33**, 659 (1986).

⁵Shoudan Liang, Phys. Rev. Lett. **64**, 1597 (1990).

⁶M. Marcu, in *Quantum Monte Carlo Methods*, edited by M. Suzuki (Springer-Verlag, Berlin, 1987), p. 64.

⁷M. Suzuki, Commun. Math. Phys. **51**, 183 (1976); M. Barma and B. S. Shastri, Phys. Rev. B **18**, 3351 (1978); J. E. Hirsch, D. J. Scalapino, R. L. Sugar, and R. Blankenbecler, Phys. Rev. B **26**, 5033 (1982).

⁸We have tested our method on four-site chains. With no assumption about eigenvalues, broad peaks are produced near $\omega/J = 0, 1, 2$, and 3. By assuming $S(q, \omega)$ is nonzero only at the exact eigenvalues, then we obtain intensities within 4% of the exact values.

⁹R. N. Silver, D. S. Sivia, and J. E. Gubernatis, in *Quantum Simulations of Condensed Matter Systems*, edited by J. D. Doll and J. E. Gubernatis (World Scientific, Singapore, 1990), p. 340.

¹⁰S. F. Gull and J. Skilling, IEEE Proc. F **131**, 646 (1984).

¹¹The treatment of the correlation between different τ values and details of the error propagation will be presented elsewhere [J. E. Gubernatis, R. N. Silver, D. Sivia, and M. Jarrell (unpublished)].

¹²P. C. Hohenberg and W. F. Brinkman, Phys. Rev. B **10**, 128 (1974).

¹³This method of default model generation was suggested by R. S. Silver after an earlier presentation of some of this work [J. Deisz, M. Jarrell, and D. L. Cox, Bull. Am. Phys. Soc. **35**, 595 (1990)].

¹⁴S. R. White has provided a comparison to our results using two other methods (unpublished).

¹⁵Y. Endoh *et al.*, Phys. Rev. Lett. **32**, 170 (1974).

¹⁶M. Marcu and J. Müller, Phys. Lett. A **119**, 469 (1987).